Thickness and Interfacial Roughness Changes in Polymer Thin Films during X-Irradiation

Andrew G. Richter,*,†,§ Rodney Guico,‡ Ken Shull,‡ and Jin Wang†

Advanced Photon Source, Argonne National Laboratory, Argonne, Illinois 60439, and Department of Materials Science, Northwestern University, Evanston, Illinois 60208

Received January 11, 2005; Revised Manuscript Received December 21, 2005

ABSTRACT: Despite the obvious occurrence of synchrotron X-ray damage to organic thin films, few attempts have been made to qualitatively determine changes to their structural parameters during X-ray exposure. We report here the use of X-ray reflectivity to study X-radiation damage to thin films of poly(*tert*-butyl acrylate) and polystyrene at various incident flux densities and sample temperatures. At the flux densities studied, (0.4−6.7) $\times$ 10^9 photons/(s mm^2), the polyacrylate film thickness decreased during irradiation at rates ranging from −0.1 to −4 Å/min, while the surface roughness increased. The volume of polymer removed per incident photon ranged from 150 to 1400 Å^3/photon. The rate of the thickness decay of the films was found to be linear with flux density over the range studied. The damage rate also appears to be directly related to the amount of X-ray energy deposited in the film, not the amount of energy available for creation of secondary electrons at the substrate. At comparable flux densities, polystyrene films heated above the glass transition temperature were found to behave similarly to the polyacrylate films, losing between 40 and 250 Å^3/photon; however, at room temperature polystyrene films instead slightly increased in thickness.

Introduction

There has been an increasing amount of interest in using synchrotron X-rays for characterizing organic thin films due to the wide variety of powerful techniques afforded by intense, well-collimated X-ray beams. Despite the weak interaction of X-rays with organic materials, including biological materials, the high brilliance afforded by synchrotron X-ray beams has facilitated many scattering and imaging methods to study these materials with fine spatial and time resolutions. In many cases, high-resolution characterization of thin films of organics has only been feasible with synchrotron X-rays. Conventionally, X-ray methods have been regarded as neither destructive nor intrusive in structural studies of a wide variety of samples. However, especially with the advent of the third-generation synchrotron sources, intense X-ray photon beams can become disruptive for organic materials.

Because X-ray photons have energies equivalent to and higher than the electron binding energies of the atoms present in organic samples, not surprisingly, many groups have reported detecting chemical changes that occur during X-ray exposure, such as loss of carbon, hydrogen, and molecular fragments, formation of carbon double bonds, incorporation of oxygen into the films, etc. For example, several systematic studies of chemical changes that occur during exposure to rotating anodes sources have been attempted mainly for assessing the effect of X-ray photoelectron spectroscopy (XPS) characterization on organic thin films.[1−8] Additionally, various groups interested in X-ray lithography have examined the effect of soft synchrotron X-rays and ultraviolet light on SAMs and polymer films.[9−15]

X-ray illumination of the substrate supporting a thin film produces secondary electrons, which have large interaction cross sections with the organic overlayers and are believed to be primarily responsible for damage in X-irradiated thin films. This mechanism implies that electron-beam-irradiated films may be damaged similarly to X-irradiated films. Because of the strong interest in the application of electron-beam lithography to organic thin films, a number of studies of electron-irradiation-induced changes have been reported,[16−27] and direct comparisons between X-ray damage and electron-beam damage have been performed.[2,13,28,29] The findings of these studies will be remarked upon in the Discussion section below.

While studies of the chemical changes that occur in organic thin films during irradiation are of fundamental importance, another significant aspect of radiation damage is changes to the film structure. As films of interest become thinner, the structure of the films increasingly influences the important properties of the films. For instance, self-assembled monolayers (SAMs), which are on the order of nanometers in thickness, are widely viewed as promising materials for many technological applications and are extensively studied using X-ray techniques. While their chemical, optical, and physical properties depend greatly on their constituent chemical compositions, without the well-ordered structure that spontaneously forms the interesting film properties would be drastically reduced. This is also true for spin-cast polymer thin films, as many research groups are presently studying the effects of film thickness on the glass transition temperature and the coefficient of thermal expansion.[30−34] Polymer films and SAMs are also used as resists for X-ray, ultraviolet, and electron beam lithography, the structural properties of which are clearly relevant. Because of the X-ray-induced structural changes in organic thin films, structures determined experimentally by using intense X-ray beams may not be representative of pristine films.

Some previous studies of radiation damage to thin films have examined the thickness using ellipsometry[10,28] and an "effective thickness" using XPS.[16−19,25,35] Of these, only one used (soft) X-rays as the irradiation source and the authors found no change in thickness.[10] However, these thickness measurements required assumptions about the film density which may not be realistic

† Argonne National Laboratory.
‡ Northwestern University.
§ Present address: Department of Physics and Astronomy, Valparaiso University, Valparaiso, IN 46393.
* Corresponding author. E-mail: Andrew.Richter@valpo.edu.

10.1021/ma050060v CCC: $33.50
Published on Web 01/27/2006

as the film becomes progressively damaged. Discussions of structural changes in thin organic films have been included in some X-ray studies, usually as side notes, but systematic studies have not be performed on the effect of synchrotron X-ray damage at typical energies used for X-ray scattering experiments.

In this paper, we present the initial results of a systematic study of the effect of synchrotron X-irradiation on the structure of ultrathin polymer films of poly(*tert*-butyl acrylate) and polystyrene at X-ray energies typically used in scattering experiments. While we will show that synchrotron X-ray characterization may not realistically be described as nondestructive, it is not our intention to suggest abandoning X-ray studies of organic thin films; rather, it is to point out the importance of understanding the limitations and complications of X-ray structural characterization and of including these concerns in data collection and analysis. These results, we hope, provide for a foundation for further work in this area so that quantitative assessments can be made regarding X-ray damage to thin organic films and mitigating procedures can be planned for and developed when necessary.

Experimental Section

Materials. Poly(*tert*-butyl acrylate) (PtBA), $[CH_2-CH-((C=O)-OC(CH_3)_3)]_n$, with a molecular weight (M_n) of 301 000 was synthesized by anionic polymerization at −78 °C in tetrahydrofuran as described elsewhere.[36] The polymer has a glass transition temperature of 49 °C, as determined by differential scanning calorimetry. PtBA thin films were prepared by spin-coating, using solutions with various concentrations of PtBA in butanol. Before the coating process, the substrates, 25 mm × 25 mm polished silicon(100) wafers, were cleaned in a boiling H_2SO_4/H_2O_2 solution (7:3 v/v), followed by extensive rinsing in deionized water. The films were coated at 2000 rpm for 40 s, resulting in thicknesses ranging from 140 to 560 Å, depending on the solution concentration. No annealing of the films was performed. All films were used within 1 week of deposition.

For the polystyrene (PS) thin films, silicon substrates were cleaned as described above, and then the oxide layer was removed by immersion in an HF/water (1:10 v/v) bath for 20 s, followed by rinsing with copious amounts of pure water. PS solutions were made using 60 000 molecular weight PS dispersed in toluene. The films were spin-coated at 2000 rpm for 40 s and then annealed in a vacuum oven for 20 h at 175 °C. Resultant films were around 450 Å in thickness.

PtBA was chosen because it is a useful polymer for X-ray studies above and below the readily accessible glass transition temperature and because our group had been using PtBA for several experiments.[37−40] PtBA is known to degrade during UV exposure or exposure to gaseous hydrochloric acid into poly(acrylic acid) by elimination of isobutene,[41,42] In general, polyacrylates degrade primarily via loss of side chains, though thermal studies show degradation via multiple channels.[43] In contrast, PS degrades through main chain scissioning and cross-linking; which channel is the dominant process varies from study to study and depends on multiple environmental parameters.[43] However, PS is used as a negative resist in X-ray and UV lithography because it cross-links and becomes insoluble.[44,45] Because of this difference in degradation pathways, the structure of PtBA and PS films should show somewhat different behaviors in reaction to X-irradiation. The exact chemical degradation pathway is not of direct concern in this paper, however. Certainly, it is the chemical changes that occur that alter the structure of the films, but the resultant changes to the structure are the primary focus in this paper.

X-ray Setup and Procedures. X-ray exposure and analysis were performed at beamline 1-BM, the bending magnet line of Sector 1, operated by X-ray Operation and Research (XOR) at the Advanced Photon Source (APS) of Argonne National Laboratory. The X-rays were monochromated to an energy of 9.659 keV using a Si(111) double crystal monochromator with sagittal focusing in the horizontal direction; the energy was calibrated by a scan through the K-adsorption edge of a zinc foil.[46] The beam was focused in the vertical direction using a bent palladium-coated mirror. The experiment was performed during four separate experimental runs denoted as runs 1−4, respectively. The exact beamline configuration varied from run to run, particularly in the degree of focusing, and therefore the slit sizes and fluxes were somewhat different in each experiment. Also, during each run, the available flux changed with time due to decay of the current in the storage ring and to refills of the storage ring. The APS has a long lifetime for the ring current, with time between fills of 12 h, the available flux dropping by ∼25% between fills. Each sample we examined was typically in the beam for 3−4 h, so the available flux usually varied around 10% for any particular sample. The incident beam was typically defined by slits to measure ∼0.2 mm vertically by 1 mm horizontally. Detector slits were set to be slightly larger to admit the entire reflected beam. Guard slits stationed just after the sample were used to reduce background, and flight paths under vacuum were used to reduce air scattering and absorption of the X-ray beam. The samples were mounted inside an enclosed chamber with Kapton X-ray windows. Using silver paste, the samples were attached to an aluminum block that contained cartridge heaters and a thermocouple for temperature control. The sample chamber was filled with a slight overpressure of helium, a standard method used to decrease air scattering of the X-rays and with the aim to lessen X-ray damage. This assumption was tested with one sample for which no helium was flowed.

X-ray reflectivity (XRR) is a powerful method for determining the structure of a film normal to the substrate. This is achieved by detecting the X-rays that reflect off the various interfaces in the film−substrate system. These reflected X-rays are coherent and so will interfere with each other. Their relative phases depend on the optical path length difference which is related to the thickness and electron density of the film and to the angle of incidence of the X-rays. The roughness of each interface will also affect the amount of the X-rays that are specularly reflected from them, changing the magnitude of the interference. Thus, by scanning over a range of incident angles, an interference pattern is obtained that contains information about the film thickness, its electron density, and the interfacial roughnesses.[47] An advantage of determining thin film thickness using the XRR technique is that the process is insensitive to the composition of the film, being dependent only on the electron density contrasts within the film.

There are several similar terms with varied meanings used to discuss radiation exposure, and so we here define the terms used in this paper. “Flux”, as it is used by synchrotron literature, is the number of photons per second in the X-ray beam. “Flux density” is the flux per unit area, having units of photons/(s mm^2). Given the nature of how synchrotron X-rays are produced, the flux density of an X-ray beam varies with time. When referring to the flux density delivered to the sample at a specific time, we will use the phrase “instantaneous flux density” to differentiate from an averaged flux density. The time-integrated (or accumulated) flux density that impinged on the samples is referred to as “fluence”, which has the units of photons/mm^2. The term “exposure” refers to the act of irradiating the samples. It should be noted that radiation damage literature commonly uses the term “dose”, generally meaning the energy absorbed by the irradiated material per unit area, and the unit “gray”, the amount of energy absorbed per unit mass. Both these terms are much better suited to studies of bulk materials, wherein direct measurements of the amount of absorbed radiation can be made, so we will not use them here.

Exposures to X-rays were typically performed as follows. First, a sample was mounted and aligned and an initial reflectivity scan was taken, exposing it to as little radiation as possible by using a beam attenuated by metal foils before the sample. Then, the sample was exposed to full beam intensity for a specified amount of time, usually 2−10 min. The measurement and exposure steps were repeated between 6 and 20 times. Because the sample size along

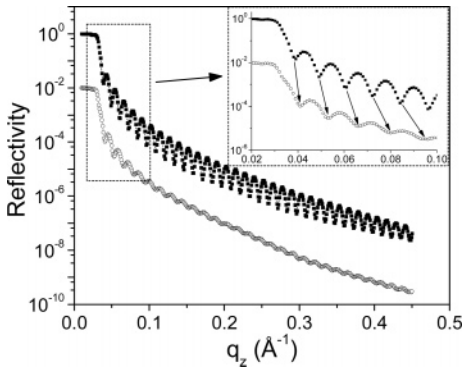

Figure 1. Reflectivity for a 499 Å PtBA film, showing the effect of X-irradiation on film structure. The upper curve (■) is for a pristine film. The lower curve (○) is for an irradiated film (fluence of 7.7 × 10^{12} photons/mm^2) and has been shifted down by a factor of 100 for clarity. q_z (= $4\pi \sin\theta/\lambda$) is the momentum transfer of the X-rays normal to the surface. There are three clear effects of radiation damage: (1) the interference oscillations become damped, (2) the overall value of the reflectivity does not change appreciably, and (3) as seen in the inset, the interference minima become more widely spaced. These changes indicate the surface of the film becomes rough and the thickness decreases.

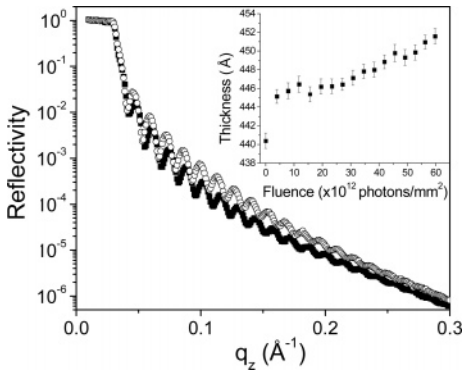

Figure 2. Reflectivity scans showing the effect of X-irradiation on a 450 Å PS film at room temperature: (■) no previous exposure and (○) after a fluence of 60 × 10^{12} photons/mm^2. In contrast to the PtBA films, PS films at room temperature increase in thickness during irradiation. The interference oscillations also increase in amplitude, and the reflectivity has a slight overall enhancement suggesting that both the film surface and film−substrate interface decrease in roughness. The inset shows the film thickness as a function of fluence.

the direction of the beam (20−30 mm) is much larger than the vertical beam size (0.2 mm), to evenly illuminate the entire sample with the X-rays the samples would be placed in the beam at a small "exposure angle", θ_{exp}, defined with respect to the surface. For most of the experiments an appropriate angle to use was 0.5°, which is above the critical angle of the film (0.128°) and at which the sample occluded 70−80% of the beam. The exposure angle was also varied to study the effect of different incident flux densities. For all exposure angles, the beam was never completely occluded, so the samples were always evenly illuminated during the exposures.

Because we used X-rays to both characterize the films and to purposefully damage the films, some complications to this procedure do arise. Although we attempted to minimize the sample exposure during the reflectivity scans—by using some attenuation in the beam throughout the scans and accepting worse statistics and a lower reciprocal space maximum than in a typical reflectivity study—a certain amount of exposure is necessary for good resolution. In any case, a complete analysis of the fluence received by a sample during both the purposeful exposure steps and the reflectivity scans was made by rigorously tabulating the incident flux, which changes over time due to the decay of the electron current in the synchrotron storage ring, and the X-ray footprint on the sample, which changes during scanning. For most cases, the fluence due to the purposeful exposures accounted for a large majority of the total fluence.

Additional methods of structural characterization, such as ellipsometry and AFM, might help to corroborate the findings of this study. We did perform AFM studies initially, but because they cannot be done in situ, we could not rule out the possibility that changes to the film structure, such as surface relaxation, might occur during the few days between X-ray exposure and AFM characterization, leading to ambiguous results. Second, as discussed below, our main structural parameter of interest is the film thickness, which cannot be ascertained using AFM because there would be no sharp boundaries between exposed and unexposed regions due to the fact that the X-ray beam profile is not a step-function. Similarly, ellipsometry measurements would be difficult to perform in situ and would not give model-free results. Therefore, we focus in this paper only on X-ray reflectivity results.

Results

Figure 1 shows two reflectivity curves for a PtBA film of about 500 Å thickness. The top reflectivity scan was taken before any exposure had occurred. The lower curve, shifted down by a factor of 100 for clarity, is after several exposures and reflectivity scans were made. There are several clear effects due to X-irradiation. There is a suppression of the size of the interference fringes (Kiessig fringes) which can most easily be explained by a corresponding increase in at least one of the interfacial roughnesses and a decrease in the film electron density. The fact that the curve does not have a significantly lower overall reflectivity implies that only one interface has broadened, and it is most likely the film−air interface. The inset of Figure 1 shows the other effect: the interference fringe interval becomes larger as evidenced by the progressive shift of the minima to higher values in q_z (= $4\pi/\lambda \sin\theta$). An increase in the period of the interference corresponds to a decrease in the film thickness. Thus, a qualitative analysis of the effect of X-irradiation on the structure of a PtBA film shows that the film loses material and the surface becomes roughened. PS films at room temperature do not show this same behavior; instead, the films become slightly thicker and less rough (see Figure 2) as evidenced a shift of the minima to lower q values, an increase in the amplitude of the oscillations, and a larger reflectivity at large q values. The inset of Figure 2 shows how the thickness changes with fluence: there is an initial jump of 5 Å, followed by a slow increase that did not saturate within the fluence range studied.

Although the reflectivity curves yield the thickness rather readily, reflectivity data must be fit to a model of the electron density for a full treatment of the structure of the film.[48,49] Some effort in this direction has been taken, and we find support for the qualitative analysis above; for example, one sample shows an increase in the film−air interface roughness from 9.3 to 24.2 Å and a decrease in the film density of 9.4% after a fluence of 5.5 × 10^{12} photons/mm^2. However, as an initial quantitative analysis of the film structure, we have chosen to focus on the main structural parameter, film thickness, which can be obtained without resorting to detailed modeling and its attendant assumptions. A simple method for finding the film thickness to high accuracy is to examine the positions of the interference minima. The thickness of a single, uniform slab of material on a substrate is related to the position of an interference minimum in the reflectivity by

$$\frac{(2n-1)\pi}{T} = \sqrt{q_n^2 - q_c^2} \qquad (1)$$

where T is the film thickness, n is a positive integer index

numbering the minima, q_n is the momentum transfer value at the nth minimum, and q_c is the critical momentum transfer for total external reflection, which depends on the film electron density. Rewriting this in terms of q_n gives

$$q_n = \sqrt{\left(\frac{(2n-1)\pi}{T}\right)^2 + {q_c}^2} \tag{2}$$

A fit of eq 2 to a plot of the minima positions vs the minima indices gives T and q_c. Note that q_c is quite small (PtBA has $q_c \approx 0.022$ Å^{-1} for 9.659 keV X-rays); therefore, for most minima, the q_c term can be safely ignored, and eq 2 can be written as a linear equation

$$q_n = \frac{2\pi}{T} n - \frac{\pi}{T} \tag{3}$$

with a slope of $2\pi/T$ and an intercept of $-\pi/T$. Only minima close to q_c will show a deviation from a straight line, which consequently also indicates that any fit to eq 2 will only have a well-determined value for q_c if there are many minima near q_c.

These equations assume a simple film, one with only two interfaces and no internal structure. Any internal interfaces will give rise to additional modulations of the reflectivity curve, complicating this simple procedure. However, if the internal interfaces are weak, that is, if there are only small electron density gradients at these interfaces compared to the gradient between the substrate and film or the film and the air, then the scattering from them is also small, and the presence of these weak interfaces will not appreciably affect this type of analysis.[30] The influence of extra interfaces that scatter strongly can be easily detected in reflectivity curves and especially in their Fourier transforms. Reflectivity scans of pristine PS and PtBA films show only the possibility of one much weaker interface; therefore, it is possible to obtain reliable values for the film thickness using eq 2 or 3. Some of the damaged films show evidence of an additional interface, presumably from a region of the sample that has experienced a substantially different fluence due to the reflectivity scans and therefore has a different thickness. In these cases, care was taken to fit only the minima that arise from regions of the sample that have experienced similar fluences, typically only the higher indexed minima representing the middle area of the sample, which receives the most fluence and the largest flux densities due to the way the X-ray footprint changes during scans.

The precision of the thickness value obtained from the minima-position method is very good because the position of each minimum is generally knowable to within one data interval, although this becomes less true for the higher ordered minima where scatter in the data becomes comparable to the signal. For an undamaged 500 Å PtBA film, we can tabulate the positions of about 30 minima, each with a very small error, leading to a well-determined thickness value with an uncertainty typically on the order of ±0.3 Å. Thinner films have fewer minima, so their thicknesses are less precisely measured. A shortcoming of this method is that when the oscillations become completely damped due an increase in surface roughness due to radiation damage, the minima positions become indeterminate. This happens to the higher q minima first, since the dampening factor goes as $\exp(-q^2\sigma^2)$ where σ is the surface roughness. So, as a film becomes thinner and rougher due to radiation damage, eventually the number of determinable minima decreases and the measured film thickness becomes less precise, limiting this analysis to smaller fluences or to films for which surface roughness does not increase rapidly during irradiation.

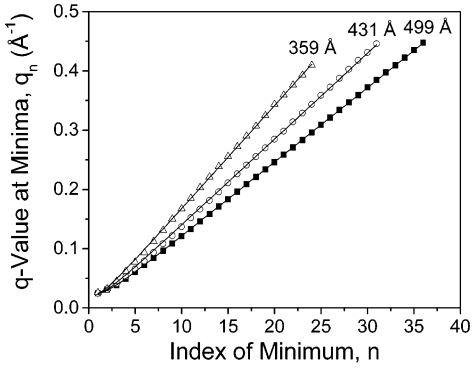

Figure 3. Minima positions for a 499 Å PtBA film after irradiation: (■) no previous exposure; (○) after 7.7×10^{12} photons/mm^2; (△) after 17.1×10^{12} photons/mm^2; and (—) fits to eq 2. As the film thickness decreases due to X-irradiation, the minima positions become more widely spaced, so the slope of the minimum position vs minimum index increases.

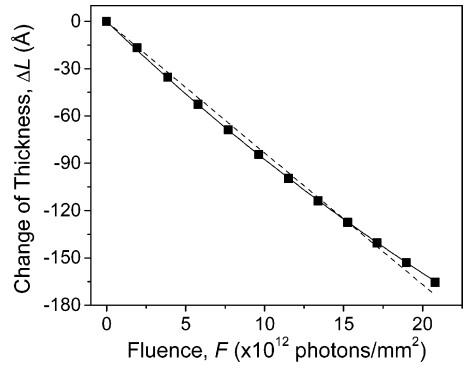

Figure 4. Change of thickness vs fluence for a 499 Å PtBA film exposed at 0.5° and a flux density of 6.73×10^9 photons/(s mm^2). The error bars are roughly 1/8 of the size of the data symbols and are therefore not shown. The thickness change is approximately linear (- - -) with a slope of $D_F = 8.34 \pm 0.01$ Å/F_0. However, a fit to the saturated exponential form given in eq 4 is clearly more appropriate (—), with $\sigma = (1.93 \pm 0.01) \times 10^{-16}$ cm^2 and ΔL_∞ taken to be the entire film thickness ($\chi^2 = 1.25$).

Figure 3 shows fits to the minima positions using eq 2 for a pristine 500 Å PtBA film and for the same film after a few exposures. Figure 4 shows the results from fitting the minima for each reflectivity scan using eq 3 for this sample. We plot the change in thickness vs the fluence. For each of the experiments, the flux density of the beam was measured for a range of storage ring currents and then linearly extrapolated to 100 mA, the maximum ring current. The flux density at the sample for any ring current at any exposure angle could then be calculated. The sample for which data are shown in Figure 4 had a flux density of 8.0×10^9 photons/(s mm^2) at an exposure angle of 0.5° at 100 mA ring current. Each exposure was not made at the maximum ring current, so the instantaneous flux densities during the exposure steps were always less than this value. The fluence that the sample received during each reflectivity scan before the current scan was also calculated and added to that received during the intentional exposures.

Two fits to these data are shown in Figure 4. We find a reasonable linear fit with a slope of -8.32 (± 0.01) $\times 10^{-12}$ Å/(photon mm^2). For ease of discussion, we will refer to the decay of thickness per unit of fluence as D_F and the thickness decay rate per unit time as D_t and define an standard fluence of $F_0 = 10^{12}$ photons/mm^2, so that the above decay rate can be

Table 1. Data for 500 Å PtBA and 450 Å PS Films

run	thickness[a] (Å)	θ_{exp} [b] (deg)	flux density (10^9 photons/(s mm^2))	D_F [c] (Å/F_0)	D_t [d] (Å/min)	σ [e] (10^{-16} cm^2)
PtBA						
4	495.6	0.05	0.67	−1.78	−0.07	
3	507.5	0.1	0.40	−1.46	−0.04	
4	498.2	0.1	0.83	−2.83	0.14	
4	475.8	0.3	2.85	−13.81	−2.36	2.90
4	484.4	0.4	4.33	−11.60	−3.01	2.40
1	493.8	0.5	1.15	−6.27	−0.43	1.27
3	499.0	0.5	2.45	−8.03	−1.18	1.61
3	498.7	0.5	2.92	−8.53	−1.49	1.71
4	498.4	0.5	6.73	−9.62	−3.88	1.93
PS (125 °C)						
4	453.8	0.5	7.22	−2.56	−1.11	4.03
4	442.7	1.5	17.17	−0.41	−0.42	0.83

[a] Initial film thickness. [b] Angle at which the sample was exposed, defined from the substrate surface. [c] The initial change of thickness per unit fluence (F_0 is an arbitrary standard of 10^{12} photons/mm^2). The volume of material removed per incident photon (in Å^3/photon) can be calculated by multiplying D_F by 100. [d] The initial change of thickness per unit time at the particular flux density. [e] The damage cross section found by fitting the thickness decay to a saturated exponential, eq 4 in the text.

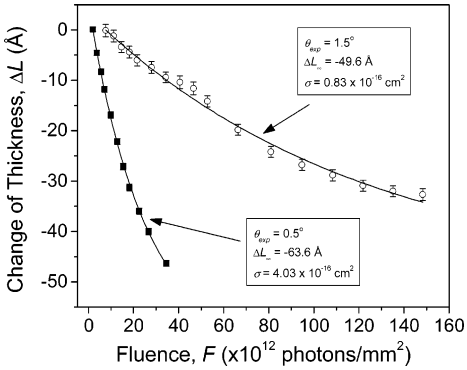

Figure 5. Change of thickness in 450 Å polystyrene films held at 125 °C at two different exposure angles, 0.5° (■) and 1.5° (○). The solid lines are fits to the saturated exponential form given in eq 4. At elevated temperatures, PS films behave similarly to PtBA films in response to X-irradiation.

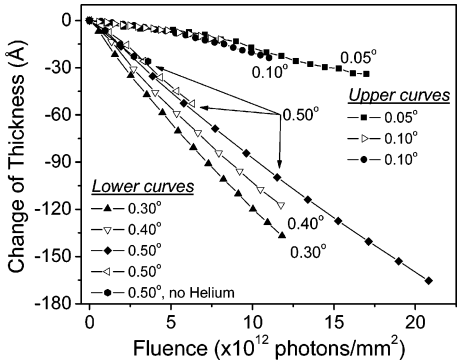

Figure 6. Thickness change vs fluence for all the PtBA films irradiated at different exposure angles. Films exposed at 0.5° all show approximately the same response to X-irradiation. Below the critical angle of the film (0.129°), the film still becomes damaged but at a slower rate. As the exposure angle increases between the critical angle and 0.5°, the rate of film thickness loss diminishes.

written as $D_F = -8.32$ Å/F_0. Multiplying this by the instantaneous flux density received by the film during the first intentional exposure gives the rate of change in thickness $D_t = -3.36$ Å/min (at 6.73×10^9 photons/(s mm^2)). The thickness decay is clearly nonlinear, however, so the data were also fit to a saturated exponential form as will be discussed below and as is shown in Figure 4. For small fluence an initial linear thickness decay rate can be found from $\sigma\Delta L_\infty$, giving $D_F = -9.62$ Å/F_0 and $D_t = -3.88$ Å/min. Other samples show similar behavior (see below). Note that D_F is also a measure of the volume of material removed from the film for each incident photon: in Å^3/photon, the volume of material removed is simply D_F multiplied by 100. Performing this calculation, we obtain values ranging from 146 to 1381 Å^3/photon, depending on exposure angle and incident flux density.

While PS films at room temperature (30 °C) did not show a loss of film thickness during irradiation, they did when held above T_g. Upon heating films to 125 °C and exposing them to X-irradiation, similar behavior to PtBA films was found (see Figure 5). Since the fluence range was larger for these PS films, the nonlinear thickness decay rate is more apparent. The thickness decay was well fit using a saturated exponential form as described in the Discussion section. At low fluence, the linear decay rate was found to be $D_F = -2.56$ Å/F_0 or $D_t = -1.11$ Å/min (at 7.22×10^9 photons/(s mm^2), $\theta_{exp} = 0.5°$), about one-quarter the rate for room temperature PtBA at the same exposure angle and similar flux density. The volume of PS removed per incident photon is also lower, ranging from 41 to 256 Å^3/photon, showing that PS is more resistant to X-irradiation than PtBA, even when heated above T_g.

In an attempt to quickly and easily control the magnitude of the flux density impinging on the samples, we varied the exposure angle—the flux density varies as sin θ_{exp}. All of the 500 Å PtBA samples exposed at 0.5° exhibit similar values for D_F (see Figure 6 and Table 1). At $\theta_{exp} = 0.05°$ and 0.10°, the thickness decay is considerably slower. Interestingly, samples irradiated at intermediate angles show larger thickness loss for similar fluences, the opposite dependence as might first be expected since the smaller the angle, the smaller the flux density. The reasons for this will be explored in the Discussion section. Exposure angles greater than 0.5° could only be achieved by using smaller samples which has certain experimental disadvantages, especially for spin-coated films: areas near the edges of a sample tend to have different thicknesses than the rest of the film and are more susceptible to dewetting. Only one film, a PS film, was exposed at greater than 0.5°.

Normally, helium is flowed over the sample in order to minimize damage due to oxidation. This has the additional benefit of lessening the loss of X-ray intensity due to air scattering. To determine whether the presence of helium actually decreases the rate of thickness loss in polymer thin films, a PtBA sample was exposed as described above but without flowing helium through the sample chamber. Within the range of fluence that the sample received, a very similar thickness decay rate was seen as compared to the samples in which helium was used (⬢ in Figure 6), although the surface did appear to roughen

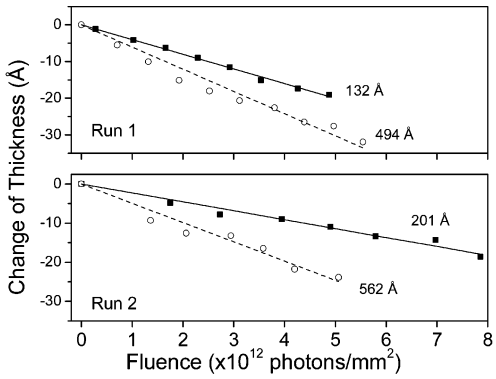

Figure 7. Thinner PtBA films degrade less than thicker films for the same fluence. The lines are linear fits to the data.

faster, making thickness measurements at high fluences impossible.

All of the PtBA samples for runs 3 and 4 were on the order of 500 Å thick. In runs 1 and 2, several thinner films were examined as well. Unfortunately, because the reflectivity scans were performed differently in the earlier runs and because other measurements such as diffuse-scattering scans were interspersed with the exposures and reflectivity scans, direct comparisons between the results from early data and from later data are problematic. However, comparisons can be safely made between data from the same run. The top part of Figure 7 shows the results for a 132 Å film and a 494 Å film. The bottom part shows the results for a 201 Å film and a 562 Å film. It is clear from this figure that thinner films decay more slowly than thicker films.

Discussion

The results shown in Figures 1, 3, and 4 demonstrate the changes that occur to the structure of thin spin-cast films of PtBA during X-irradiation: the film loses material, becoming thinner, and the surface becomes rougher. While the exact value of the roughness increase must be determined from more complete analyses than shown in this paper, the loss of thickness is readily apparent and calculable using a simple minima position fitting routine. The different response to X-irradiation of PS films at room temperature, as shown in Figure 2, is likely related to radiation-induced cross-linking, lowering the density and increasing the thickness, assuming the amount of film material is conserved. Chain fragments would be less likely to be formed or to escape the cross-linked polymer network below T_g, where the mobility of chain fragments is low. Frey et al. found that SAMs containing aromatic groups were much more resistant to low-energy electron damage than aliphatic SAMs, attributing this resistance to cross-linking between aromatic groups and delocalization of the radiation-induced excitation over the extended $\pi-\sigma$ system.[26] Above T_g, chain fragments are more free to migrate to the surface and escape the film, so PS films held above T_g respond to X-irradiation similarly to PtBA films at room temperature. It should be noted that the loss of film thickness cannot be due to thermal contraction caused by heating of the film and substrate due to absorption of X-ray energy: we observed that both types of films thermally expand, rather than contract, when heated.

At small fluences, the thickness decrease of PS films held above T_g and of PtBA films is fairly linear, giving decay rates ranging from -0.4 Å/min to almost -4.0 Å/min at flux densities typical of focused bending magnet lines at third-generation synchrotrons at grazing incident angles. The rate of thickness loss for each sample decreases as the fluence increases. Figure 7 demonstrates that initially thinner films decay slower than initially thicker films, indicating that the reduction in the thickness decay rate may be due to a film thickness effect. The following sections will discuss the concept of a damage cross section for thickness loss, examine the various possible causes of the film thickness effect, and finally combine these analyses with the exposure angle variation results.

Damage Cross Section. Several groups have observed a loss of SAM film thickness due to electron irradiation, measuring the film thickness with XPS[16−19,25] and ellipsometry.[28] They found that the thickness decrease is initially quick and then saturates to some minimum film thickness—typical thickness loss is on the order of 20−40% of the initial film thickness. A formalism used by these authors is to fit the change in thickness to a saturation function

$$\Delta L = \Delta L_\infty[1 - \exp(-\sigma F)] \quad (4)$$

where ΔL is the change in thickness after an fluence of F electrons/cm^2, ΔL_∞ is the maximal change in thickness, and σ is an electron "damage cross section", a measure of the rate at which the thickness decreases with electron fluence. Applying eq 4 to the data in Figure 4, we calculate a cross section of 1.93 ($\pm$0.01) $\times$ 10^{-16} cm^2 for a 500 Å PtBA film. Zharnikov found a value of 1.84 $\times$ 10^{-16} cm^2 for low-energy electron damage to alkylthiol SAMs on Au substrates.[25] The fact that our value is so similar to Zharnikov's is probably coincidence, but because it is within the same order of magnitude, it indicates that the damage done by grazing incidence 9.659 keV X-ray photons is equivalent to that done by normally incident 10 eV electrons. Using a variety of techniques, others researchers have found other damage cross sections for other irradiation-induced effects with similar values,[7,11,19,21,22] mainly involving chemical changes, such as loss of hydrogen, formation of carbon double bonds, and loss of end groups. For PtBA films we do not observe a saturation of thickness loss at values near 20−40%, which would correspond to a maximal thickness change of 100−200 Å for a 500 Å film, within or near the range that we examined. However, the maximal change in thickness for the PtBA films is somewhat poorly determined since the total fluence was small compared to $1/\sigma$ and the saturation value of the thickness was not approached; when allowed to vary, ΔL_∞ becomes close to, or even greater than, the full film thickness. Fixing a value for ΔL_∞ within the 20−40% range does not give good fits. Therefore, when finding σ for PtBA films, ΔL_∞ is set to be the same as the initial film thickness for all fits to eq 4; the results of these fits are shown in Table 1.

If the main damage channel for PtBA is assumed to be loss of side groups, then the maximal thickness loss should be $5/9L_0$, or -277 Å for $L_0 = 499$ Å as was found by Esker when exposing PtBA films to gaseous hydrochloric acid.[42] Fits to the data with this assumption are not reasonable—the curve noticeably does not go through the data points, and the reduced χ^2 is 62. Therefore, loss of side groups alone is likely not the sole damage channel for PtBA unless eq 4 is not valid. If ΔL_∞ does not equal the full film thickness, then the damage cross sections given in Table 1 for PtBA films are lower limits. For fits with different values for ΔL_∞ with reduced χ^2 up to 10, σ increases by about 35%, while $D_F = -\sigma\Delta L_\infty$ increases by just 5%. PS films heated to 125 °C, on the other hand, were irradiated with fluences comparable to $1/\sigma$, and therefore ΔL_∞ was allowed to vary in the fits, giving values of 10−15% of the initial film thickness, indicating that PS films cross-link extensively enough to retain most of their material.

Table 2. Exposure Angle Dependence of Thickness Decay Rates for the PtBA Films from Run 4

θ_{exp} [a] (deg)	Λ_z [b] (μm)	$1 - \exp(-L/\Lambda_z)$ [c]	$(1 - R)$ [d]	A [e]	A_{norm} [f] (%)	D_F [g] (Å/F_0)	D_{F-norm} [h] (%)
0.05	0.0046	1	0.001	0.001	4	−1.78	19
0.1	0.0063	1	0.003 54	0.003 54	14	−2.83	29
0.3	11.131	0.041 777	0.995 00	0.041 61	170	−13.81	144
0.4	15.676	0.030 403	0.998 20	0.030 35	124	−11.60	121
0.5	20.057	0.024 523	0.999 78	0.024 52	100	−9.62	100

[a] Angle at which the sample was exposed, defined from the substrate surface. [b] The attenuation length along the surface normal. [c] The amount of an X-ray beam absorbed within a film after transiting its thickness, L. [d] The amount of incident beam transmitted into the film. [e] The amount of energy absorbed within the film relative to the incident energy. [f] The absorbed energy normalized to the absorbed energy at an exposure angle of 0.5°. [g] D_F, as given in Table 1. [h] D_F for each exposure angle normalized to D_F at an exposure angle of 0.5°. The correlation between the normalized values of A and D_F suggests that direct absorption of energy within the film is primarily responsible for film thickness loss.

Film Thickness Effect on the Thickness Decay Rate. In this section, we will present some discussion about reasons for the film thickness effect. The main cause of damage to organic films from X irradiation has been posited to be due to secondary electrons generated within the substrate (and, to a much lesser extent, within the film).[4,11,35,50] These electrons have energies of around 10 eV and path lengths of only 10−40 Å.[16,18,23,35] Thus, as far as damage from electrons is concerned, there should be no difference between films that are 200 Å thick and films that are 500 Å thick since both capture the majority of the electrons' energy. However, we see a marked difference in the degree of damage between films of these thicknesses, so it is difficult to explain the faster film thickness decay rate for thicker films on the basis of damage from secondary electrons generated within the substrate.

Several groups have observed that electron damage of SAMs is stronger for longer molecular chains (thicker films) than for short chains.[1,4,24,27] This has been explained using dissociative electron attachment (DEA) theory with the increase in damage arising due to the decrease in the lifetime of a non-chain-breaking deexcitation pathway as a function of distance from the substrate.[16,24,27] The effect relies on the coupling of an excitation dipole in the chain terminus with an image dipole created in the metal substrate. For our samples, the image dipole−excitation dipole interaction will be much weaker due to the nonmetallic substrate, and therefore the effect due to film thickness will be greatly reduced. Additionally, the excitation dipole orientation at a noncrystalline polymer film surface should be isotropic, further reducing the dipole−dipole interaction strength.

Several groups have found that irradiated organic film material changes into a carbonaceous form which could have a different response to irradiation.[1−3,19,20,28] Additionally, irradiation can induce the formation of highly cross-linked species with a subsequently shorter mean free path for chain fragments and a lower probability of production of fragments because more bonds must be broken simultaneously, both which would reduce decay rates.[1,3,20] However, we have found that even thinner *pristine* films show reduced damage rates, and therefore irradiation-induced changes such as these cannot completely explain our results.

Koch et al. investigated the damage occurring in organic electroluminescent thin films from vacuum-ultraviolet (VUV) radiation from an undulator beamline with a flux density 2 orders of magnitude higher than that in our experiment.[15] They observed that thicker films degraded more than thinner films. They attributed this to increased surface charging of thicker films, although the same films exposed to radiation from a bending magnet beamline, with similar intensities as in our experiment, showed no degradation at all. Another group exposed 100 Å thick PMMA films to VUV and found no evidence for surface charging.[14] Surface charging is expected to increase disorder in films near the surface and by this mechanism to slow the loss of chain fragments from the film.[1] Since our polymer films are already disordered at the surface, it is not clear what effect surface charging, if it indeed is occurring for our films, would have on the film thickness decay rate.

Finally, the path length of X-rays within a film is directly proportional to the thickness. The attenuation of X-rays is related exponentially to the path length within the medium, so more X-ray energy will be absorbed within thicker films. After examining the above possibilities, direct absorption of X-rays within the film best explains both the slowdown in thickness decay rate as the films get thinner and the slower decay rate seen for thinner pristine films. The dependence of the thickness decay rate on the exposure angle (see below) also suggests that the damage is primarily caused by direct absorption within the film.

Exposure Angle Dependence. The incident flux density varied due to the differing beam intensities between runs and was intentionally changed by adjusting the exposure angle. The exposures of PtBA with the highest incident flux densities were obtained at an exposure angle of 0.5° during run 4. Figure 6 and Table 1 show the results for this and lower flux densities. The lowest angles, 0.05° and 0.1°, which are below the critical angle of the film (0.128°) and the substrate (0.185°), show slower thickness decay rates, as might be expected since nearly 100% of the beam is reflected from the film surface. The exposures done at 0.3° and 0.4° show an increased rate of thickness loss, D_F, despite the smaller flux densities and the (slightly) lower amount of transmission into the film, opposite to what might be expected. We can explain this most simply by calculating the amount of X-ray energy absorbed during the beam transit through the film at different exposure angles. The fraction of the incident energy absorbed within the film is

$$A \equiv \frac{E_{abs}}{E_{inc}} = (1 - R)(1 - e^{-L/\Lambda_z}) \qquad (5)$$

where L is the film thickness, R is the reflectivity of the film surface, and Λ_z is the X-ray attenuation length normal to the surface, obtained from the CXRO website (http://www-cxro.lbl.gov/optical_constants/atten2.html) and assumed to be similar to PMMA. The ratio of the absorption at $\theta_{exp} = 0.3°$ and 0.4° to that occurring at 0.5° is calculated to be 170% and 124%, respectively, varying approximately as the inverse of the ratio of the exposure angles. For exposures done below the critical angle (0.05° and 0.1°), almost all of the photons are reflected from the surface, but the attenuation length is very small so that all the energy that enters the film is absorbed, leading to a value that is 4% and 14% of the absorption at 0.5°, respectively. We find reasonable agreement between these calculated ratios and the ratios of D_F at the respective exposure angles to D_F at 0.5° (see Table 2), though the observed ratios are larger for 0.05° and 0.1° and smaller for 0.3°. At the lowest exposure

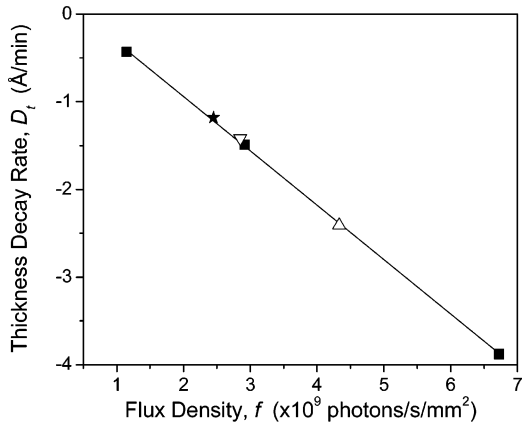

Figure 8. PtBA film thickness decay rate, in Å/min, for different initial flux densities for $\theta_{exp} = 0.5°$ (■). Over this limited range, the thickness decay rate is linear with flux density (—), with a slope of approximately −0.01 Å/s, for every 10^9 photons/(s mm^2) that impinge on the sample. The open symbols are for samples exposed at 0.3° (▽) and 0.4° (△) after angle normalization. The star symbol (★) is the sample exposed at 0.5° without helium, showing that the presence of helium does not mitigate the loss of film material.

angles, the flux density is very small so that the X-ray reflectivity scans are responsible for an equivalent amount of the received fluence, leading to a faster thickness decay rate than expected from the above analysis. Note that for 0.3° and higher the grazing-incidence enhancement of the electric field within the film is negligible—the enhancement drops precipitously above the critical angle. Also, these exposure angles are well beyond the range of incidence angles that give rise to a resonance enhancement of the electric field within the film due to the X-ray standing wave effect.[51]

If we can extrapolate our limited data to arbitrary θ_{exp}, we observe that the absorption within the film is proportional to $1/\sin\theta_{exp}$, leading to smaller values of D_F at larger θ_{exp}. On the other hand, for the same beam intensity, the flux density is proportional to $\sin\theta_{exp}$, effectively compensating for the lower absorption when determining D_t. Therefore, for exposures above the critical angle, we expect that for a given beam flux (1) exposures done at higher angles damage the film less than at lower angles when receiving the same fluence and (2) the thickness loss per minute is independent of exposure angle. An implication of this analysis is that the rate of thickness loss is related directly to the X-ray photon absorption within the film, not to the remaining photon intensity at the substrate, and consequently is independent of secondary electrons from the substrate. This analysis also relates directly to the film thickness effect discussed above, since thinner films absorb less X-ray energy.

The direct relation that we observe between the absorption within the film, A, and D_F can explain why the thickness decreases according to eq 4. For small values of L/Λ_z, which is the case for films less than 1 μm thick and for all exposure angles larger than several times the critical angle, eq 5 simplifies to $A = L/\Lambda_z$, since R quickly becomes vanishingly small. If we set $D_F \equiv dL/dF = -CA = -CL/\Lambda_z$, where C is some interaction volume, and solve for $L(F)$, we recover the exponential form for the change in thickness given in eq 5, where $\sigma = C/\Lambda_z$.

Figure 8 shows the time rate of change of the thickness, D_t, for 500 Å PtBA films taken during the different runs. Since each run was performed at different beam intensities, a range of instantaneous flux densities impinged on the samples. The data are described very well by a straight line, indicating that the damage rate (Å/min) is linear with flux density, at least over this limited range. The slope of the linear fit is approximately −0.01 Å/s for every 10^9 photons/(s mm^2) that impinge on the sample or about 1000 Å^3 of polymer removed per incident photon. The data for the 0.3° and 0.4° exposure angles are also located on this line when modified by multiplying by $\sin(0.3°)/\sin(0.5°)$ and $\sin(0.4°)/\sin(0.5°)$, respectively.

One of the data points in Figure 8 is from a sample that was exposed in ambient atmosphere, not under helium (★). The fact that the linear thickness decay rate is similar to the other samples exposed at 0.5° shows that the presence of helium does not appear to alter the rate at which material is removed from the sample. However, the sample did show a faster increase in roughness, as evidenced by a rapid dampening of the reflectivity oscillations (data not shown). That the lack of helium did not affect the rate at which material was removed from the PtBA film may be understood by the resistance of PtBA to photo-oxidation. More studies will need to be performed to fully address this point.

Conclusions

Using X-ray reflectivity, we have examined the changes that occur to the structure of thin PtBA and PS films during X-irradiation. Qualitative examination of the reflectivity curves shows that for PtBA films at room temperature and for PS films above T_g the thickness decreases and the air/film interfacial roughness increases. At the flux densities examined and at room temperature, PS films increase slightly in thickness and show a decrease in interfacial roughness. Because film thickness can be obtained from reflectivity data in a model-independent manner, we have chosen to focus on that parameter. We have found that for exposures performed above the critical angle the decrease in thickness is approximately linear, with values ranging from −0.4 to −4.0 Å/min, depending on the incident flux density. We also find values for the damage cross section ranging between 0.8×10^{-16} and 4×10^{-16} cm^2, in close agreement to those found by others using electron beam and X-ray irradiation. Thinner films are found to damage more slowly than thicker films. The volume of material removed from the films per incident photon was found to range from 150 to 1400 Å^3/photon for PtBA films at room temperature and 40 to 260 Å^3/photon for PS films at 125 °C, depending on incident flux density and exposure angle, indicating that PS is more resistant to film material loss than PtBA. The damage rate appears to be related to the amount of X-ray energy absorbed directly by the film, not the amount of energy available at the substrate for the production of secondary electrons. Since the flux density and the X-ray attenuation length have compensating dependencies on the exposure angle, the thickness decay rate per unit time is independent of exposure angle, while the thickness decay rate per unit fluence is larger for smaller angles, above the critical angle. Finally, purging the sample chamber with helium does not lessen the rate at which the PtBA film thickness decreases.

Despite the occurrence of X-ray-induced damage to polymer thin films, X-ray characterization of the structure of polymer films remains an indispensable tool and will continue to provide valuable information, especially as the films of interest become thinner. This study should in no way be taken to imply that X-ray evaluation of polymer thin films should not be performed. Rather, it must be acknowledged that X-ray damage does occur and must be accounted for or that methods must be used to minimize its effects.

Acknowledgment. Beamline support by the Sector 1 staff at the Advanced Photon Source is greatly appreciated. This work

and the use of the Advanced Photon Source are supported by the U.S. Department of Energy, BES-Materials Science, under Contract W-31-109-ENG-38.

References and Notes

(1) Frydman, E.; Cohen, H.; Maoz, R.; Sagiv, J. *Langmuir* **1997**, *13*, 5089−5106.
(2) Rieke, P. C.; Baer, D. R.; Fryxell, G. E.; Engelhard, M. H.; Porter, M. S. *J. Vac. Sci. Technol. A* **1993**, *11*, 2292−2297.
(3) Wagner, A. J.; Han, K.; Vaught, A. L.; Fairbrother, D. H. *J. Phys. Chem. B* **2000**, *104*, 3291−3297.
(4) Zerulla, D.; Chassé, T. *Langmuir* **1999**, *15*, 5285−5294.
(5) Suzuki, N.; Isano, T.; Sakamoto, T.; Saino, T.; Iimura, K.-I..; Kato, T. *Surf. Interface Anal.* **2000**, *30*, 301−304.
(6) Buncick, M. C.; Thomas, D. E.; McKinny, K. S.; Jahan, M. S. *Appl. Surf. Sci.* **2000**, *156*, 97−109.
(7) Perry, C. C.; Wagner, A. J.; Fairbrother, D. H. *Chem. Phys.* **2002**, *280*, 111−118.
(8) Wagner, A. J.; Carlo, S. R.; Vecitis, C.; Fairbrother, D. H. *Langmuir* **2002**, *18*, 1542−1549.
(9) Moon, J. H.; Kim, K.-J.; Kang, T.-H.; Kim, B.; Kang, H.; Park, J. W. *Langmuir* **1998**, *14*, 5673−5675.
(10) Kim, T. K.; Yang, X. M.; Peters, R. D.; Sohn, B. H.; Nealey, P. F. *J. Phys. Chem. B* **2000**, *104*, 7403−7410.
(11) Heister, K.; Zharnikov, M.; Grunze, M.; Johansson, L. S. O.; Ulman, A. *Langmuir* **2001**, *17*, 8−11.
(12) Yang, X. M.; Peters, R. D.; Kim, T. K.; Nealy, P. F.; Brandow, S. L.; Chen, M.-S.; Shirey, L. M.; Dressick, W. J. *Langmuir* **2001**, *17*, 228−233.
(13) Rightor, E. G.; Hitchcock, A. P.; Ade, H.; Leapman, R. D.; Urquhart, S. G.; Smith, A. P.; Mitchell, G.; Fischer, D.; Shin, H. J.; Warwick, T. *J. Phys. Chem. B* **1997**, *101*, 1950−1960.
(14) Okudaira, K. K.; Morikawa, E.; Hasegawa, S.; Sprunger, P. T.; Saile, V.; Seki, K.; Harada, Y.; Ueno, N. *J. Electron Spectrosc. Relat. Phenom.* **1998**, *88*−*91*, 913−917.
(15) Koch, N.; Pop, D.; Weber, R. L.; Böwering, N.; Winter, B.; Wick, M.; Leising, G.; Hertel, I. V.; Braun, W. *Thin Solid Films* **2001**, *391*, 81−87.
(16) Zharnikov, M.; Geyer, W.; Gölzhäuser, A.; Frey, S.; Grunze, M. *Phys. Chem. Chem. Phys.* **1999**, *1*, 3163−3171.
(17) Heister, K.; Frey, S.; Gölzhäuser, A.; Ulman, A.; Zharnikov, M. *J. Phys. Chem. B* **1999**, *103*, 11098−11104.
(18) Völkel, B.; Gölzhäuser, A.; Müller, H. U.; David, C.; Grunze, M. *J. Vac. Sci. Technol. B* **1997**, *15*, 2877−2881.
(19) Müller, H. U.; Zharnikov, M.; Völkel, B.; Schertel, A.; Harder, P.; Grunze, M. *J. Phys. Chem. B* **1998**, *102*, 7949−7959.
(20) Hutt, D. A.; Leggett, G. J. *J. Mater. Chem.* **1999**, *9*, 923−928.
(21) Rading, D.; Liebing, V.; Becker, G.; Fuchs, H.; Benninghoven, A. *J. Vac. Sci. Technol. A* **1998**, *16*, 3449−3454.
(22) Werst, D. W.; Vinokur, E. I. *J. Phys. Chem. B* **2001**, *105*, 1587−1593.
(23) Lamont, C. L. A.; Wilkes, J. *Langmuir* **1999**, *15*, 2037−2042.
(24) Olsen, C.; Rowntree, P. A. *J. Chem. Phys.* **1998**, *108*, 3750−3764.
(25) Zharnikov, M.; Frey, S.; Heister, K.; Grunze, M. *Langmuir* **2000**, *16*, 2697−2705.
(26) Frey, S.; Rong, H.-T.; Heister, K.; Yang, Y.-J.; Buck, M.; Zharnikov, M. *Langmuir* **2002**, *18*, 3142−3150.
(27) Huels, M. A.; Dugal, P.-C.; Sanche, L. *J. Chem. Phys.* **2003**, *118*, 11168−11178.
(28) Seshadri, K.; Froyd, K.; Parikh, A. N.; Allara, D. L.; Lercel, M. J.; Craighead, H. G. *J. Phys. Chem.* **1996**, *100*, 15900−15909.
(29) La, Y.-H.; Kim, H. J.; Maeng, I. S.; Jung, Y. J.; Park, J. W. *Langmuir* **2002**, *18*, 301−303.
(30) Thompson, C.; Saraf, R. F.; Jordan-Sweet, J. L. *Langmuir* **1997**, *13*, 7135.
(31) Lin, E. K.; Kolb, R.; Satija, S. K.; Wu, W.-L. *Macromolecules* **1999**, *32*, 3753−3757.
(32) Müller-Buschbaum, P.; Staum, M. *Macromolecules* **1998**, *31*, 3686−3692.
(33) Fryer, D. S.; Peters, R. D.; Kim, E. J.; Tomaszewski, J. E.; de Pablo, J. J.; Nealy, P. F.; White, C. C.; Wu, W.-L. *Macromolecules* **2001**, *34*, 5627−5634.
(34) Weber, R.; Zimmermann, K.-M.; Tolan, M.; Stettner, J.; Press, W.; Seeck, O. H.; Erichsen, J.; Zaporojtchenko, V.; Strunskus, T.; Faupel, F. *Phys. Rev. E* **2001**, *64*, 061508 (5 p).
(35) Graham, R. L.; Bain, C. D.; Biebuyck, H. A.; Laibinis, P. E.; Whitesides, G. M. *J. Phys. Chem.* **1993**, *97*, 9456−9464.
(36) Ahn, D.; Shull, K. R. *Macromolecules* **1996**, *29*, 4381.
(37) Guico, R. S.; Narayanan, S.; Wang, J.; Shull, K. R. *Macromolecules* **2004**, *37*, 8357−8363.
(38) Cole, D. H.; Shull, K. R.; Baldo, P.; Rehn, L. *Macromolecules* **1999**, *32*, 771−779.
(39) Cole, D. H.; Shull, K. R.; Rehn, L. E.; Baldo, P. *Phys. Rev. Lett.* **1997**, *78*, 5006−5009.
(40) Cole, D. H.; Shull, K. R.; Rehn, L. E.; Baldo, P. M. *Nucl. Instrum. Methods Phys. Res. B* **1998**, *136*−*138*, 283−289.
(41) Monahan, A. R. *J. Polym. Sci., Part A-1* **1966**, *4*, 2381−2390.
(42) Esker, A. R.; Mengel, C.; Wegner, G. *Science* **1998**, *280*, 892−895.
(43) Bandrup, J.; Immergut, E. H. *Polymer Handbook*, 3rd ed.; John Wiley & Sons: New York, 1989.
(44) Schnabel, W.; Sotobayashi, H. *Prog. Polym. Sci.* **1983**, *9*, 297−365.
(45) Thurn-Albrecht, T.; Schotter, J.; Kastle, G. A.; Emley, N.; Shibauchi, T.; Krusin-Elbaum, L.; Guarini, K.; Black, C. T.; Tuominen, M. T.; Russel, T. P. *Science* **2000**, *290*, 2126.
(46) Lang, J. C.; Srajer, G.; Wang, J.; Lee, P. L. *Rev. Sci. Instrum.* **1999**, *70*, 4457−4462.
(47) Gibaud, A. Specular Reflectivity from Smooth and Rough Surfaces. In *X-ray and Neutron Reflectivity: Principles and Applications*; Daillant, J., Gibaud, A., Eds.; Springer: Berlin, 1999.
(48) Tolan, M. *X-Ray Scattering from Soft-Matter Thin Films*; Springer: Berlin, 1999.
(49) Tidswell, I. M.; Ocko, B. M.; Pershan, P. S. *Phys. Rev. B* **1990**, *41*, 1111−1127.
(50) Laibinis, P. E.; Graham, R. L.; Biebuyck, H. A.; Whitesides, G. M. *Science* **1991**, *254*, 981−983.
(51) Wang, J.; Bedzyk, M. J.; Caffrey, M. *Science* **1992**, *258*, 775−778.

MA050060V